

Physical and Numerical Evaluation of a Geosynthetic Reinforced Soil Wall with Concave Facing Profile

D. Stathas, Division of Infrastructure and Transportation, EBP Switzerland AG, Zürich, Switzerland
J.P. Wang, Department of Civil Engineering, National Central University, Zhongli, Taiwan
H.I. Ling, Department of Civil Engineering & Engineering Mechanics, Columbia University, New York, USA
L. Xu, Department of Civil Engineering & Engineering Mechanics, Columbia University, New York, USA
L. Li, Department of Civil Engineering & Engineering Mechanics, Columbia University, New York, USA

ABSTRACT

Geosynthetic reinforced soil walls (GRSWs) offer an environmental-friendly and low-cost solution to earth retaining structures. GRSWs are usually built with a planar facing profile and only few studies have investigated the effects of profile geometry on the wall performance. Several studies based on analytical solutions suggested that a concave geometry could improve the stability of a slope or reduce the tensile forces acting on the reinforcement layers of a GRSW. This study investigated the performance of a concave GRSW compared to planar ones based on physical modelling (centrifuge tests with 1:10 scale) and numerical models using the finite element method. The results of this study show that a concave wall can significantly reduce the mobilized tensile force (up to 27%), when the soil is at a critical state (low friction angle) and the reinforcement is of low stiffness. For a higher soil internal friction and stiffer reinforcement, the advantage of concave geometry is insignificant. In summary, this study provides physical and numerical evidence showing that the concave GRSWs are more stable than planar ones. Last but not least, another highlight of this study is that we utilized 3D printing to fabricate block miniatures in building a concave wall model.

1. INTRODUCTION

1.1 Geosynthetic reinforced soil walls (GRSWs) and wall geometry

Geosynthetic reinforced soil walls are proven to be a sustainable solution (Damians et al. 2018) to earth retaining problems with increasing popularity. The current design guidelines seem to overestimate the tension in reinforcement and the accurate prediction of reinforcement loads has been an interesting and ongoing research topic in the past years (Allen and Bathurst 2015, Bathurst et al. 2019, Leshchinsky et al. 1995, 2014). The main elements of a GRSW are backfill soil, geosynthetic reinforcement and facing elements. The interaction among these elements creates a complex system and its performance is influenced by many factors. Research work conducted in the past and based on physical or numerical data, investigated parameters such as soil strength (Ling et al. 2012), reinforcement and (Bathurst et al. 2009) facing stiffness (Bathurst et al. 2006). The scope of the previous studies was to provide a better understanding and optimized design for GRSWs for the parameters mentioned.

The wall geometry (batter angle) can also have a significant effect on the reinforcement loads. GRSWs are commonly designed with a planar profile, vertical or inclined, and only limited research work (Vahedifard et al. 2016a) has investigated the influence of geometry on GRSW performance. Studies based on analytical solutions have shown that slopes or reinforced soil walls with concave profile are more stable than planar slopes (Jeldes et al. 2015, Utili and Nova 2007, Vahedifard et al. 2016b). Vahedifard et al. (2016a) proposed a design concept referred to as middle chord offset (MCO), to assist the optimal design of a reinforced soil structure with a concave profile. However, the analytical solutions discussed earlier are based on simplified assumptions and do not consider the deformational behavior of the system. The scope of this study is to investigate the performance of concave GRSW based on numerical data from elastoplastic analysis with simplified models (Mohr-Coulomb) used widely by practical engineers. The numerical analysis and input parameters were validated with physical data, acquired by centrifuge testing.

1.2 Porcupine Blocks and 3D-printing

The facing of a GRSW can be hard or soft and its stiffness affects the structure's performance (Ehrlich and Mirmoradi 2013, Tatsuoka 1993). The construction of a concave geometry with a hard facing from concrete blocks can be quite challenging in practice. To overcome this difficulty, porcupine blocks (Figure 1), a modular block with unique geometry features (curved surface and multiple interlocking), were used in this research work to enable the construction of a curved geometry. The manufacturing of accurate miniature blocks for centrifuge testing was another challenge for this study. 3D-Printing technology has been recently used in geotechnical physical modelling (Hanaor et al. 2016, Stathas et al. 2017) and was implemented successfully for the production of the miniature blocks in the current study as well. Details about block manufacturing are presented by Stathas et al. (2018) and will not be discussed further in the current paper.

2. PHYSICAL MODELING

2.1 Centrifuge models tests

2.1.1 Wall geometry

Centrifuge testing is widely used in geotechnical research (Balakrishnan and Viswanadham 2016, Ling et al.2016). The reliability of centrifuge testing is based on scaling laws (Garnier et al. 2007) to simulate accurately the performance of full-scale systems with small models. The current study used 1:10 (scale factor: $N = 10$) model tests to examine the behavior of two 3.0 m high GRSWs with a batter angle of 18° . The first model (PRSW18) was designed with a planar profile as benchmark and the second with concave (CRSW18) facing geometry. The geometry of the concave profile was determined according to the MCO concept (Vahedifard et al. 2016a). The soil was reinforced with three geogrid layers (RF1 bottom, RF2 middle, RF3 top) and each layer was equipped with three strain gauges (SG1 to SG9). Figure 1 shows the model wall configuration for the two GRSWs and the porcupine block used to construct them.

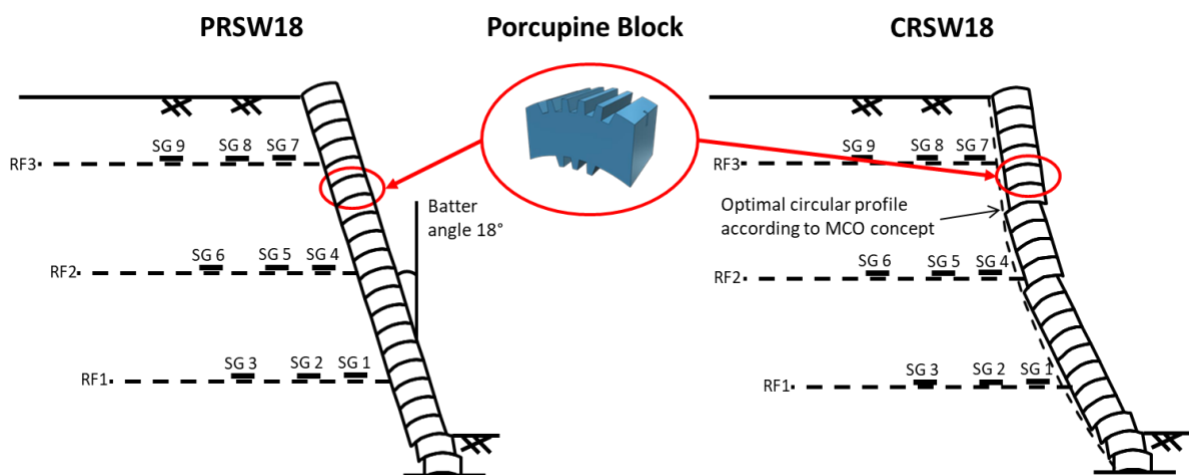


Figure 1. GRSW models

2.1.2 Block and soil properties

The shape of the miniature block was slightly modified, compared to the original full-scale block. The full-scale block has dimensions of 15x20x30 cm and weights 20 kg. Each dimension was scaled down 10 times ($1/N$) according to scaling laws of centrifuge testing (1.5x2.0x3.0 cm). The model blocks were 3D-printed with PLA material and filled with lead balls to meet scaling mass requirements ($1/N^3$). The final model block weight was 0.02kg with an average density of 2.2g/cm^3 .

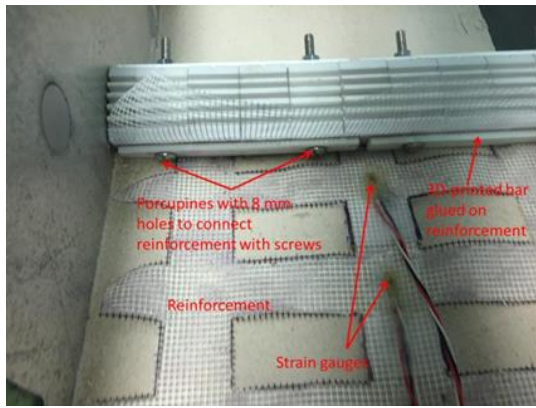
The soil used in the current study was Nevada sand available at the centrifuge facility of Columbia University in the city of New York with its properties summarized in Table 1.

Table 1. Nevada sand properties

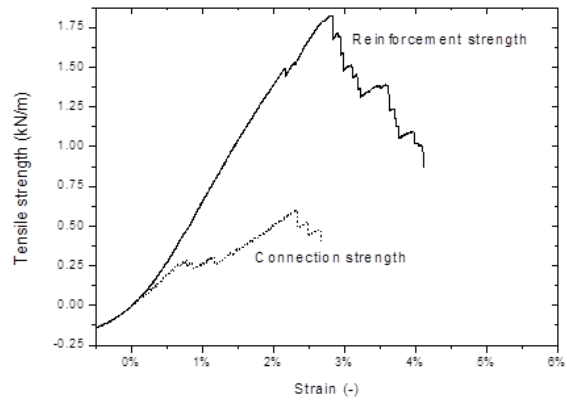
Nevada sand	Density ρ (g/cm^3)	Friction angle ϕ ($^\circ$)	Dilation angle ψ ($^\circ$)	Specific gravity G_s (g/cm^3)	Average grain size d_{50} (mm)	Water content w (%)
<i>Foundation</i>	1.718	33	5	2.67	0.15	5
<i>Backfill</i>	1.636	33	3	2.67	0.15	5

2.1.3 Soil Reinforcement and instrumentation

The model reinforcement was a mosquito net with openings 2.2 x 2.2 mm. It was connected by 3D-printed bars and steel screws on the porcupine blocks (Figure 2a) to simulate a use-case block-reinforcement connection (Ling et al. 2000) from the practice. The tensile strength of reinforcement and the connection were tested according to ASTM 6637 and they are shown in Figure 2b. Part of the reinforcement in the model was removed to adjust its tensile strength ($EA = 69\text{ kN/m}$) and simulate a common full-scale geogrid. Strain gauges were glued on reinforcement to record the tensile force (through stain readings) during testing. The strain gauges were placed at 0.1, 0.3 and 0.5L, where L is the reinforcement length.



a) Block reinforcement connection



b) Reinforcement and connection strength

Figure 2. Properties of model reinforcement: a) Configuration of reinforcement connection. Mosquito net connected with facing blocks using bolts and 3D printed bars. b) Tensile strength of model reinforcement (1,75kN/m) and reinforcement-block connection (0,50kN/m). Failure at 3% strain for both cases

2.2 Performance of physical models

The models were built in a rigid box (50/20/48 cm) and tested at the centrifuge facility of Columbia University. The models were submitted gradually to a centrifugal acceleration up to 10g. After reaching the desired g-level, uniform surcharge load was applied at the top of the structure and increased 25 kPa per minute until the model fails (observation of large deformation). The strain gauge readings were recorded during testing and used later to estimate the tensile load on the reinforcement.

CRSW18 failed as the surcharge load was increased from 50 to 75 kPa. Similarly PRSW18 failed when load was increased was from 75 to 100 kPa. In both cases, the failure mode was rupture of top reinforcement layer (RF3) at block-reinforcement connection.

3. NUMERICAL MODEL VALIDATION

3.1 Numerical Model

A numerical analysis was also conducted to further investigate further the performance of the two wall models. The analysis was conducted with Finite Element Method (FEM) and OptumG2 was used as analysis software. The geometry of FEM model was identical to the physical one scaled up 10 times. The mesh size was set to 0.075 m. Figure 2 shows the FEM model including details of connection between reinforcement and facing block.

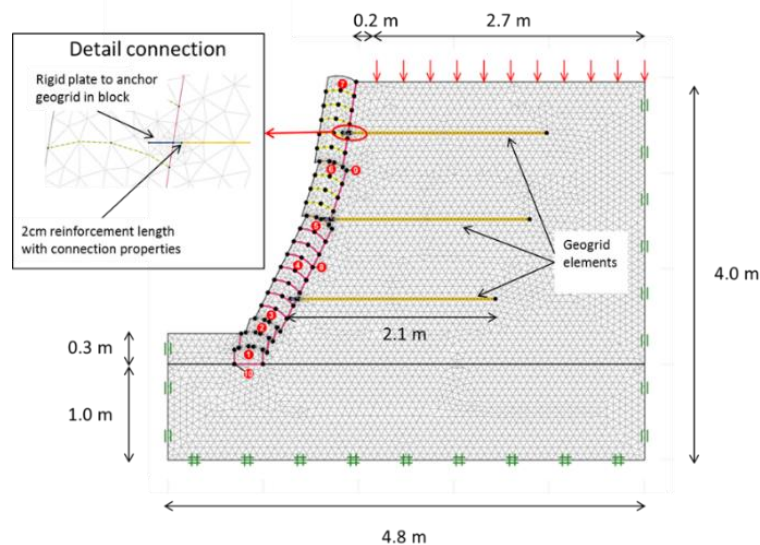


Figure 3. Numerical validation model

The soil model for this study was a linear elastic model with Mohr-Coulomb (MC) failure criteria because of its simplicity and broaden use in practice. The soil's internal angle of friction under plane strain conditions (ϕ_{ps}) was estimated from

direct shear tests (φ_{ds}) and Eq. 1 (Allen et al. 2003). A cohesion of 0.5 kPa was used to simulate the apparent cohesion in soil due to the 5% water content. Soil-block and block-block interfaces were also modeled as linear elastic - MC materials with strength properties estimated from direct shear tests. The reinforcement and the connection were modeled as an elastoplastic element with tensile strength scaled up 10 times according to the tensile tests presented earlier (Figure 2a). Table 2 summarizes the material properties used for the finite element analysis.

$$\varphi_{ps} = \text{atan}(1.2 \tan(\varphi_{ds})) \text{ in degrees}$$

[1]

Table 2. Element properties for numerical model

Element	Model ¹	Unit weight γ (kN/m ³)	Friction angle φ (°)	Cohesion c (kPa)	Young's Mod. E (MPa)
Soil Backfill	MC	16.05	41.0	0.5	20
Soil	MC	16.85	43.0	0.5	20
Foundation/ Embedment					
Soil-Block interface	MC	0.00	22.0	0.0	20
Block-Block interface	MC	0.00	4.0	28.0	0.005 – 0.013 ²
			Interface reduction strength factor r (-)	Yielding strength n_p (kN/m)	Axial stiffness EA (kN/m)
Geogrid	EP	0.00	0.9.	17.5	690
Connection	EP	0.00	0.9.	5	200

¹ MC: Linear elastic with Mohr-Coulomb failure criteria and EP: Elastoplastic

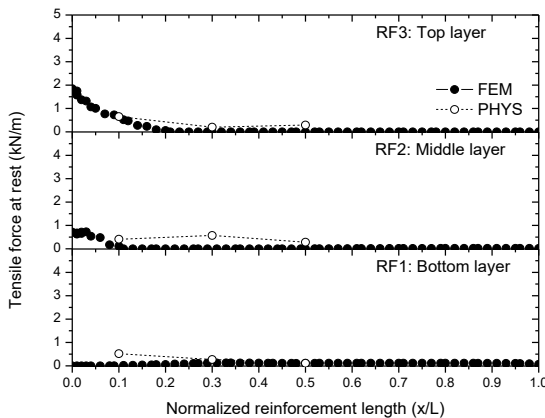
² Shear Modulus G (MPa)

3.2 Numerical analysis

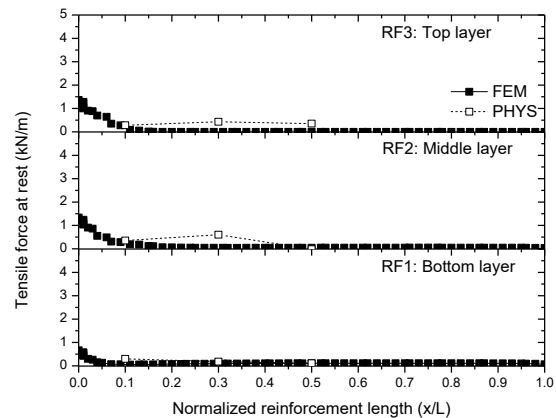
3.2.1 Reinforcement loads

The initial stresses were generated by the gravity load option available in OptumG2. The surcharge load applied on the top of the backfill was 25 and 50 kPa. Figure 4 shows the tensile forces along the reinforcement for each loading stage, including the initial stage (no surcharge loading). In the same Figure are shown the tensile forces from physical models for direct comparison. Note that the loads from physical models are scaled up with a factor of 10 to be compatible with the numerical data.

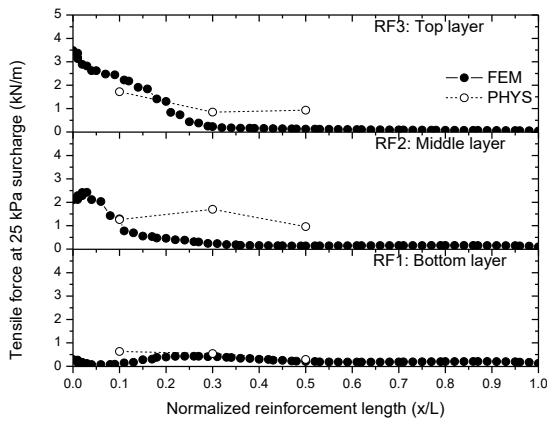
Like other research work comparing physical and numerical data (Yu et al. 2016), small discrepancies also appear in this study. These discrepancies could be attributed to the simplicity of the model used to describe the material behavior and/or to effects such as the bending of strain gauges, which influence the accuracy of the physical data. As Figure 4e shows the connection load for CRSW18 at 50kPa (if scaled down with $N=10$) is close to the strength of the block-reinforcement connection, this could explain why CRSW18 failed when the surcharge load exceeded the 50 kPa. The same observation was made for PRSW18 when the surcharge load exceeded 75kPa. Hence, through the numerical data, it was possible to validate the failure mechanism observed in the physical model tests. Overall, the comparisons of the load data from numerical analysis and physical model tests are in good agreement with each other and tend to capture the distribution and the magnitude of the tensile forces.



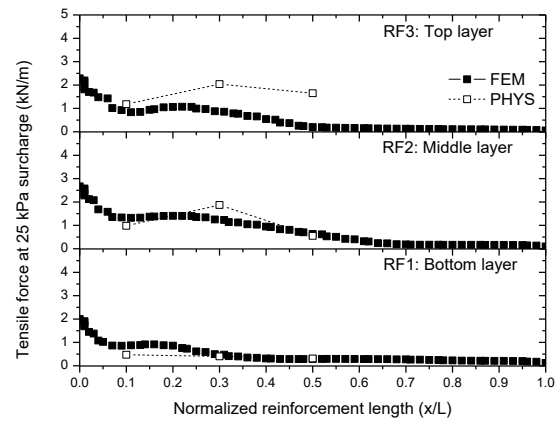
a) CRSW18 at 0kPa



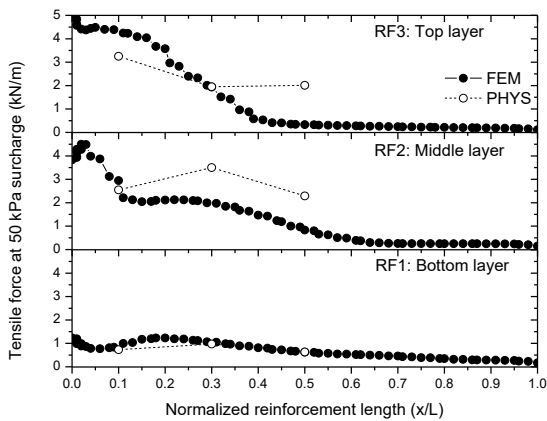
b) PRSW18 at 0kPa



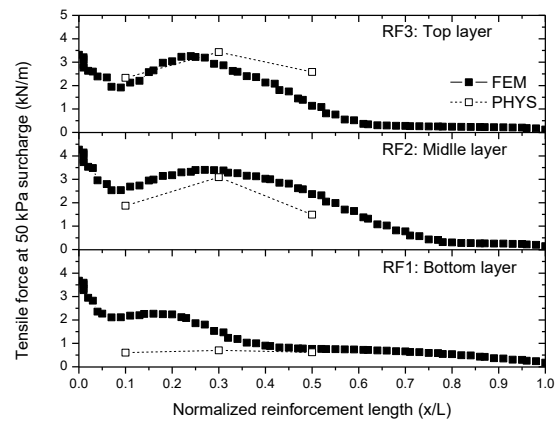
c) CRSW18 at 25kPa



d) PRSW18 at 25kPa



e) CRSW18 at 50kPa



f) PRSW18 at 50kPa

Figure 4. Tensile forces in reinforcement at different loading stages for planar (PRSW18) and concave (CRSW18) model. FEM shows tensile forces from finite element model, whereas PHYS is used to describe the data acquired from the centrifuge tests (scaled-up with factor $N = 10$)

3.2.2 Model evaluation

Similar to other studies (Hatami and Bathurst 2006, Yu et al., 2016) two peak values appear at every reinforcement layer. The first value is at the connection point of block-reinforcement (connection load: CL) and the second within the backfill soil (reinforcement load: RL) at a distance larger than $0.1L$, where L is the reinforcement length.

CL appeared already at 0 kPa surcharge load (Figs. 4a and 4b) when the backfill-soil is stable and the reinforcement is still inactive. CL can be attributed to drag-down forces due to the relative settlement of the backfill soil behind the hard facing. As the surcharge load increases, the backfill-soil becomes unstable and the reinforcement is activated to support it. Tensile forces are being developed along the reinforcement resulting in the second peak value (RL) shown in Figures 4c to 4f. Part of the RL is transferred to the facing while loading is increasing. Hence, the resulting CL is the summation of drag-down force at connection point and part of RL.

The top reinforcement layer (RF3) was proven to be critical for CRSW18 with higher loads than PRSW18. The middle (RF2) and bottom (RF3) layers of CRSW18 have significantly lower RF compared to PRSW18. As Table 3 shows, for CRSW18 the summation of RL (7.69kN/m) is almost 14% lower than for PRSW18 (8.93kN/m). This indicates a higher factor of safety for concave profiles concerning the overall system stability. However, CRSW18 has a lower safety factor concerning the geogrid strength (higher CL und max RL).

Table 3: Reinforcement loads from numerical models

Tension loads from FEM model (kN/m)	max CL	max RL	Summation of RL
CRSW18	5	4.5	7.69
PRSW18	4.25	3.5	8.93

3.3 Parametric analysis

The validated numerical model will be used to investigate the influence of soil strength, reinforcement stiffness, and soil-block interface properties. The parametric model was slightly modified compared to the validation model. The surcharge load used in the parametric study was 10 kPa and the block-foundation soil friction angle was assumed to be $\phi_{BB, Found} = 43^\circ$ (e.g. assuming a leveling pad from gravel under base block and fully rough surface of base block). These assumptions were made to eliminate any effect resulting from the variation of toe resistance or due to excessive surcharge load. Moreover, these two assumptions as well as the variation of parameters are realistic for a retaining wall design in practice. The connection was also assumed be able to mobilize the full strength of the geogrids by using another type of connection (e.g. geogrid connectors). Table 4 summarizes the values used in the parametric study.

Table 4: Variables for parametric model

	Properties	Values
Soil backfill	Friction angle ϕ ($^\circ$)	30, 32.5, 35, 37.5, 40
	Cohesion c (kPa)	0.1
Interface of block-soil	Friction angle ϕ_{sb} ($^\circ$)	0, $\phi/3$, $2\phi/3$, ϕ
	Cohesion c (kPa)	0.1
Geogrid	Yielding strength n_p (kN/m)	16, 142
	Axial stiffness (kN/m)	160, 1420
Connection		geogrid properties

3.4 Results of parametric study

3.4.1 Soil strength and reinforcement stiffness

The sum of RL shows the necessary total force to stabilize the GRSW under service conditions (soil is not at critical state). Hence, the performance of the two geometries could be evaluated with respect to the sum of RL (ΣRL). Figure 5a shows that the use of low stiffness reinforcement (EG16) and low strength soil ($\phi = 30^\circ$) can reduce the ΣRL up to 27%. As the soil strength increases, the geometry does not influence the system performance under service loads. The use of a very stiff reinforcement (T120RE) reduces the effect of geometry as well. As it is shown in Figure 5b, for low strength soil ($\phi = 30^\circ$) and high stiffness reinforcement (T120RE), the ΣRL is 20% less for concave profile. Figure 6 shows the influence of block and backfill-soil friction (δ) on the system's performance. A rough block-backfill soil interface (high values of δ) increases the ability of the facing to transfer load and reduces the reinforcement loads (ΣRL). The use of very stiff reinforcement (T120RE) and fully rough interface ($\delta = \phi$) shows no difference between concave and planar profile.

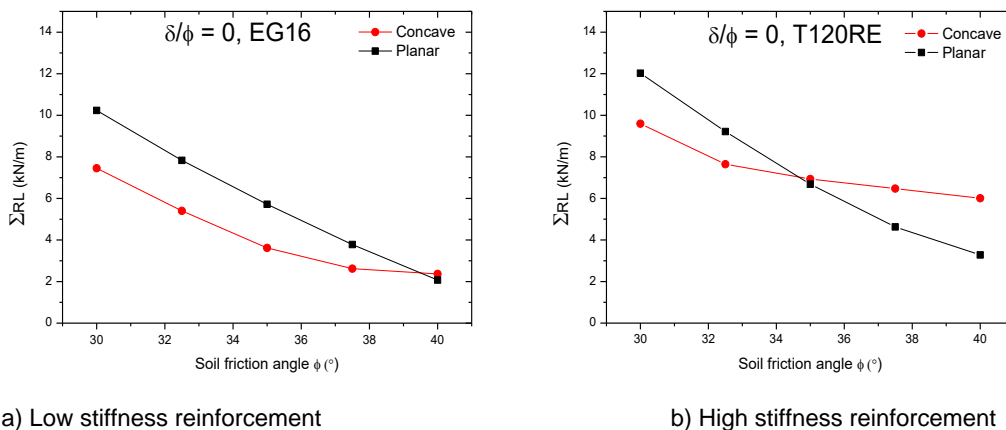


Figure 5. Variation of soil friction angle and reinforcement stiffness.

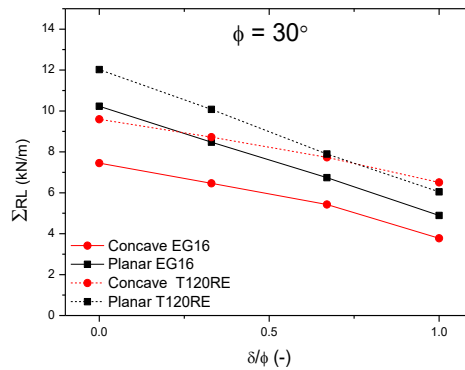


Figure 6. Variation of block-backfill soil friction

4. SUMMARY AND CONCLUSIONS

The current study investigated the effect of a concave geometry on the performance of GRSW by considering the deformational behavior of the system based on numerical analysis and centrifuge testing. The study showed that concave profile can reduce up to 27% of the reinforcement loads of a GRSW under service conditions. However, the positive effect of concave geometry is dominated from soil strength, reinforcement stiffness and friction between facing block and backfill soil. Accordingly, the conclusions can be drawn:

- Concave geometry would reduce the backfill volume of a GRSW and subsequently the construction cost of a GRSW
- Top reinforcement layer is the critical layer for a concave wall. The block-reinforcement connection needs to be designed accordingly to avoid failure of the connection
- MCO is a rational design concept to determine the optimal profile geometry
- Concave profile can assist to optimize the design of a reinforced soil wall by using reinforcement of lower stiffness and low strength backfill

REFERENCES

- Allen, T. M., Bathurst, R. J., Holtz, R. D., Walters, D. and Lee, W. F. (2003). A new working stress method for prediction of reinforcement loads in geosynthetic walls, *Canadian Geotechnical Journal*, 40: 976 - 994.
- Allen, T.M. and Bathurst, R.J. (2015). Improved Simplified Method for Prediction of Loads in Reinforced Soil Walls, *J. Geotech. Geoenviron. Eng.*, 141: 04015049.
- ASTM D6637. Standard Test Method for Determining Tensile Properties of Geogrids by the Single or Multi-Rib Method, *American Society for Testing and Materials*, West Conshohocken, Pennsylvania, USA.
- Balakrishnan, S. and Viswanadham, B.S.V. (2016). Performance evaluation of geogrid reinforced soil wall with marginal backfills through centrifuge model tests, *Geotextiles and Geomembranes*, 44: 95 - 108.
- Bathurst, R.J., Allen, T.M., Miyata, Y., Javankhoshdel, S. and Bozorgzadeh N. (2019): Performance-based analysis and design for internal stability of MSE walls, *Georisk: Assessment and Management of Risk for Engineered Systems and Geohazards*, 13: 214-225.
- Bathurst, R.J., Nernheim, A., Walters, D.L., Allen, T.M., Burgess, P. and Saunders, D.D. (2009). Influence of reinforcement stiffness and compaction on the performance of four geosynthetic-reinforced soil walls, *Geosynthetics International*, 16: 43 - 59.
- Bathurst, R.J., Vlachopoulos, N., Walters, D.L., Burgess, P.G. and Allen, T.M. (2006). The influence of facing stiffness on the performance of two geosynthetic reinforced soil retaining walls, *Canadian Geotechnical Journal*, 43: 1225 - 1237.
- Damians, I.P., Bathurst, R.J., Adroguer, E.G., Josa, A., and Lioret, A. (2018). Sustainability assessment of earth-retaining wall structures, *Environmental Geotechnics*, 5: 187- 203.
- Ehrlich, M., & Mirmoradi, S.H. (2013). Evaluation of the effects of facing stiffness and toe resistance on the behavior of GRS walls, *Geotextiles and Geomembranes*, 40: 28 - 36.
- Garnier, J., Gaudin, C., Springman, S.M., Culligan, P.J., Goodings, D., Konig D., Kutter, B., Phillips, R., Randolph, M.F. and Thorel, L. (2007). Catalogue of scaling laws and similitude questions in geotechnical centrifuge modeling, *International Journal of Physical Modeling in Geotechnics*, 7: 01 - 23.
- Hanaor, D.A.H., Gan, Y., Revay, M., Airey, D.W., Einav, I. and (2016). 3D printable geomaterials, *Géotechnique*, 66: 323-332.
- Hatami, K. and Bathurst, R.J. (2006). Numerical Model for Reinforced Soil Segmental Walls under Surcharge Loading, *J. of Geotechnical and Geoenvironmental Engineering*, 132: 673-684.
- Jeldes, I.A., Vence, N.E. and Drumm, E.C. (2014). Approximate solution to the Sokolovskii concave slope at limiting equilibrium, *International Journal of Geomechanics*, 15: 04014049

- Leshchinsky, D., Ling, H. I. and Hanks, G. (1995). Unified Design Approach to Geosynthetic Reinforced Slopes and Segmental Walls, *Geosynthetics International*, 2: 845 - 881.
- Leshchinsky, D., Kang, B.J., Han, J. and Ling, H.I. (2014). Framework for limit state design of geosynthetic-reinforced walls and slopes, *Transp. Infrastruct. Geotechnol.*, 1: 129-164.
- Ling, H.I., Cardany, C.P., Sun, L.X. and Hashimoto, H. (2000). Finite Element Study of a Geosynthetic-Reinforced Soil Retaining Wall with Concrete-Block Facing, *Geosynthetics International*, 7: 163-188.
- Ling, H.I., Leshchinsky, D., Mohri, Y. and Wang, J.P. (2012). Earthquake response of reinforced segmental retaining walls backfilled with substantial percentage of fines, *J. Geotechnical and Geoenvironmental Engineering*, 138: 934 - 944.
- Ling, H.I., Xu L., Leshchinsky, D., Collin, J.G. and Rimoldi, P. (2016). Centrifugal modeling of geosynthetic reinforced soil retaining walls considering staged construction, *Geosynthetics, Forging a Path to Bona Fide Engineering Materials GSP 275. ASCE Geo-Chicago Conference*, Chicago, IL. USA: 95-105
- Stathas, D., Wang, J.P. and Ling, H.I. (2017). Model geogrids and 3D printing, *Geotextiles and Geomembranes*, 45: 688–696.
- Stathas, D., Xu, L., Wang, J.P., Ling, H.I. and Li, L. (2018). Concave segmental retaining walls, *Physical Modelling in Geotechnics*, Taylor & Francis Group, London, UK: 1457-1462.
- Tatsuoka, F. (1993). Roles of facing rigidity in soil reinforcing, *International Symposium on Earth Reinforcement Practice*, H. Ochiai, S. Hayashi, and J. Otani. A.A. Balkema, Fukuoka, Japan: 2: 831 - 870
- Utili, S., and Nova, R. (2007). On the optimal profile of a slope, *Soils and Foundations*, 47: 717–729.
- Vahedifard, F., Shahrokhbabadi, S. and Leshchinsky, D. (2016a). Geosynthetic reinforced soil structures with concave facing profile, *Geotextiles and Geomembranes*, 44: 358–365.
- Vahedifard, F., Shahrokhbabadi, S. and Leshchinsky, D. (2016b). Optimal profile for concave slopes under static and seismic conditions, *Canadian Geotechnical Journal*, 53: 1522-1532.
- Yu, Y., Bathurst, R.J., Allen, T.M. and Nelson, R. (2016). Physical and numerical modelling of a geogrid-reinforced incremental concrete panel retaining wall, *Canadian Geotechnical Journal*, 53: 1883–1901